AD-A124 442 DEVELOPMENTS IN LARM2: A LONGITUDINAL-VERTICAL TIME-VARYIN HYDRODYNAMIC..(U) EDINGER (J E) ASSOCIATES INC WAYNE PA J E EDINGER ET AL. JAN 83 WES-TR-E-83-1 1/1

UNCLASSIFIED DACW39-78-C-0057 F/G 9/2 NL

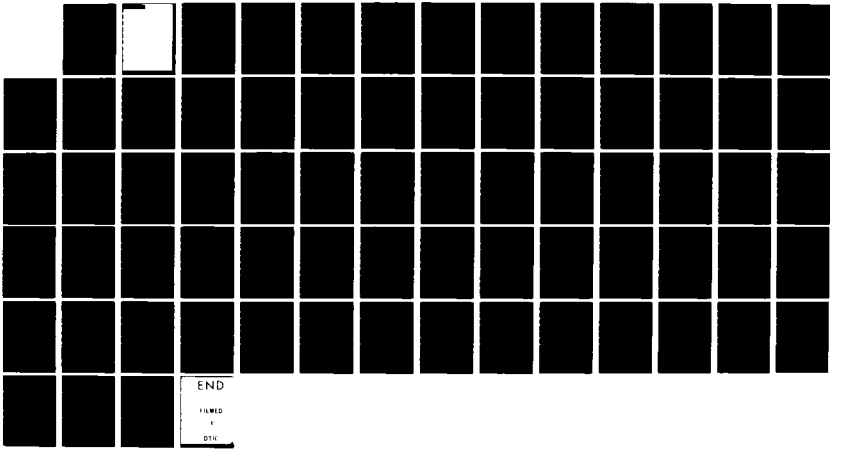

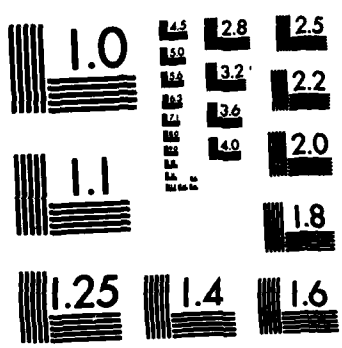

Unclassified

SECURITY CLASSIFICATION OF THIS PAGE (When Data Entered)

REPORT DOCUMENTATION PAGE

READ INSTRUCTIONS BEFORE COMPLETING FORM

1. REPORT NUMBER: Technical Report E-83-1	2. GOVT ACCESSION NO.: AD-A127 442
3. RECIPIENT'S CATALOG NUMBER	
4. TITLE (and Subtitle): DEVELOPMENTS IN LARM2: A LONGITUDINAL-VERTICAL, TIME-VARYING HYDRODYNAMIC RESERVOIR MODEL	5. TYPE OF REPORT & PERIOD COVERED: Final report
	6. PERFORMING ORG. REPORT NUMBER
7. AUTHOR(s): John E. Edinger and Edward M. Buchak	8. CONTRACT OR GRANT NUMBER(s): Contract No. DACW39-78-C-0057
9. PERFORMING ORGANIZATION NAME AND ADDRESS: J. E. Edinger Associates, Inc. 37 West Avenue Wayne, Pa. 19087	10. PROGRAM ELEMENT, PROJECT, TASK AREA & WORK UNIT NUMBERS: Work Unit 31593, Task IA.4
11. CONTROLLING OFFICE NAME AND ADDRESS: Office, Chief of Engineers, U. S. Army Washington, D. C. 20314	12. REPORT DATE: January 1983
	13. NUMBER OF PAGES: 66
14. MONITORING AGENCY NAME & ADDRESS (if different from Controlling Office): U. S. Army Engineer Waterways Experiment Station Hydraulics Laboratory P. O. Box 631, Vicksburg, Miss. 39180	15. SECURITY CLASS. (of this report): Unclassified
	15a. DECLASSIFICATION/DOWNGRADING SCHEDULE

16. DISTRIBUTION STATEMENT (of this Report)

Approved for public release; distribution unlimited.

17. DISTRIBUTION STATEMENT (of the abstract entered in Block 20, if different from Report)

18. SUPPLEMENTARY NOTES

Available from National Technical Information Service, 5285 Port Royal Road, Springfield, Va. 22151.

19. KEY WORDS (Continue on reverse side if necessary and identify by block number)

Computer programs
Hydrodynamics
LARM2 (Computer program)
Mathematical models
Reservoirs
Water quality

20. ABSTRACT (Continue on reverse side if necessary and identify by block number)

A two-dimensional, laterally averaged reservoir hydrodynamic model, LARM, was modified to provide several enhancements. The two major enhancements made to the numerical model were the incorporation of a water quality transport module (WQTM) and the capability to add or delete upstream longitudinal segments during flooding or drawdown. WQTM is a general-purpose transport algorithm for which the user must specify the water quality constituents and the constituent internal sources and sinks with the associated reaction rates.

(Continued)

DD FORM 1 JAN 73 1473 EDITION OF 1 NOV 65 IS OBSOLETE

Unclassified

SECURITY CLASSIFICATION OF THIS PAGE (When Data Entered)

20. ABSTRACT (Concluded).

Included within the report are discussion of previous LARM applications and recommendations for future development. The version of the LARM code that resulted from this effort is referred to as LARM2.

In addition to the developments reported herein, there is a user guide for LARM2 entitled "User Guide for LARM2: A Longitudinal-Vertical, Time-Varying Hydrodynamic Reservoir Model" (Buchak and Edinger, 1982).

PREFACE

The study reported herein was sponsored by the Office, Chief of Engineers, U. S. Army, as part of the Civil Works General Investigations, Environmental and Water Quality Operational Studies (EWQOS) Program. Work Unit No. 31593 (Task IA.4) entitled "Improve and Verify Multidimensional Hydrodynamic Mathematical Models for Reservoirs" supported the subject study.

The study was conducted during the period July 1978 to October 1980 by Dr. John E. Edinger and Mr. Edward M. Buchak of J. E. Edinger Associates, Inc. Mr. Mark S. Dortch and Dr. Billy H. Johnson of the Hydraulics Laboratory, U. S. Army Engineer Waterways Experiment Station (WES) monitored the effort. This report was written by Dr. Edinger and Mr. Buchak. Program manager of EWQOS was Dr. Jerome L. Mahloch, WES Environmental Laboratory.

Commanders and Directors of WES during this study and the preparation of this report were COL John L. Cannon, CE, COL Nelson P. Conover, CE, and COL Tilford C. Creel, CE. Technical Director was Mr. Fred R. Brown.

This report should be cited as follows:

Edinger, J. E., and E. M. Buchak. 1983. "Developments in LARM2: A Longitudinal-Vertical, Time-Varying Hydrodynamic Reservoir Model," Technical Report E-83-1, prepared by J. E. Edinger Associates, Inc., for the U. S. Army Engineer Waterways Experiment Station, Vicksburg, Miss.

Table of Contents

	Page
PREFACE	i
LIST OF FIGURES	iii
LIST OF TABLES	iv
1. INTRODUCTION	1.1
2. INVESTIGATIONS WITH LARM2	2.1
Center Hill Studies	2.1
Potomac Estuary Studies	2.3
Sensitivity Tests with WES GRH Flume	2.7
3. THE WATER QUALITY TRANSPORT MODULE AND CONSTITUENT SOURCE-SINK ROUTINES	3.1
Formalization of WQTM	3.2
Constituent Internal Sources and Sinks	3.7
Example - Sediment Transport	3.9
Example - Nitrogen Cycle	3.11
4. SPECIAL TOPICS IN LARM2 DEVELOPMENT	4.1
Coordinate Transforms and Bottom Slopes	4.1
Variable Longitudinal Grid	4.5
Steady-State Solution	4.7
Channel Conveyance	4.9
Reservoir Branching	4.10
Turbulence and Mixing Processes	4.12
5. RECOMMENDATIONS	5.1
Channel Conveyance	5.1
Reservoir Branching	5.2
Turbulent Kinetic Energy Transport and Mixing	5.2
Water Quality Constituent Formulations	5.3
REFERENCES	
APPENDIX A: NOTATION	A1

List of Figures

Figure Title		Page
Figure 2.1	Comparison of Observed and Predicted Tidal Ranges along the Potomac Estuary	2.11
Figure 2.2	Comparison of Observed and Predicted Tidal Phase along the Potomac Estuary	2.12
Figure 2.3	Comparison of Observed and Computed Velocities 35 km from the Estuary Mouth (Station P19) for the Indicated Depths	2.13
Figure 2.4	Computed and Observed Tidal Averaged Velocity Profile, Maximum Ebb and Flood Velocities, and Salinity Profile at Station P19 Potomac Estuary for September 9-10, 1974	2.14
Figure 2.5	Computed Vertical Dispersion Coefficients for Station P19 Hourly through a Tide Cycle Corresponding to Velocity Profiles in Figure 2.4	2.15
Figure 3.1	Nitrogen-Cycle Structure in Aerobic Aquatic Ecosystems (From Najarian and Harleman (1975))	3.15
Figure 4.1	Possible Transformed Grid Representation of Longitudinal-Vertical Reservoir Dynamics	4.17

List of Tables

Table	Title	Page
Table 2.1	Center Hill Lake Comparison of Predicted and Observed Temperatures (°C) for April 4, 1974 (Gordon, 1979)	2.16
Table 2.2	Center Hill Lake Comparison of Predicted and Observed Temperatures (°C) for September 27, 1972 (Gordon, 1979)	2.17
Table 2.3	Center Hill Lake Comparison of Predicted and Observed Temperatures (°C) for March 29, 1973 (Gordon, 1979)	2.18
Table 2.4	Center Hill Lake Comparison of Predicted and Observed Temperatures (°C) for August 15, 1973 (Gordon, 1979)	2.19
Table 3.1	FORTRAN Coding of WQTM Algorithm in LARM2	3.16
Table 3.2	Summary of RR(JC,M) Coefficients for Linear Evaluation of Nitrogen Cycle	3.18

DEVELOPMENTS IN LARM2: A LONGITUDINAL-VERTICAL, TIME-VARYING HYDRODYNAMIC RESERVOIR MODEL

1. INTRODUCTION

LARM developments for 1979-1980 include (1) modifications and refinements to produce LARM2 as presented in the User Guide (Buchak and Edinger, 1982); (2) numerous investigations with LARM2, including sensitivity analyses and testing; (3) development of a water quality transport module (WQTM) for use in multiple and interacting water quality constituent transport; (4) investigation of special topics related to LARM-type simulations, including eddy coefficient evaluation, hydrodynamic volume conveyance, and branching; and (5) recommendations for further extensions.

The USER GUIDE FOR LARM2: A LONGITUDINAL-VERTICAL, TIME-VARYING HYDRODYNAMIC RESERVOIR MODEL includes (1) the latest LARM2 modifications for upstream cell addition and subtractions and (2) surface volume addition/subtraction corrections due to depth-variable width. The code and user guide also include new routines for tributary inflow and withdrawal computations. The present report covers the remaining subject areas of LARM2 investigations, the WQTM with sediment and constituent transport as examples, and the special topics related to future LARM development.

2. INVESTIGATIONS WITH LARM2

Numerous case studies have been made with LARM2, and each has provided new insight to its applicability. A number of case studies by J.E. Edinger Associates, Inc. (JEEAI) and others are on Corps-related projects. The recent JEEAI reservoir studies are reported in the User Guide (Buchak and Edinger, 1982). The Corps related studies are by Gordon (1979), Johnson (1981), and Edinger and Buchak (1980). These studies have shown the versatility of the LARM2 computational basis and have indicated parameter sensitivity under a wide range of conditions.

The studies by Gordon (1979) of the Center Hill Reservoir include a sensitivity study as well as a seasonal temperature verification. The investigations by Johnson (1981) included simulation of an underflow density current in a Waterways Experiment Station (WES) flume and determined the parameter effects of scaling to small grid sizes of transitional laminar flows. The studies by Edinger and Buchak (1980) include the conversion of LARM2 reservoir boundary conditions to estuarine boundaries and the comparison of computed and observed velocities for tidal flows. Each of these studies has shown the sensitivity of LARM computations to different parameters under different conditions.

Center Hill Studies

Center Hill Lake near Cookeville, Tennessee, was studied by Gordon (1979) using LARM2. One purpose of the study was to verify

the ability of LARM2 to predict observed temperature distributions using only geometry, inflow, and meteorological data. Another purpose of the study was to determine the sensitivity of LARM2 velocity profiles to different types of outfall conditions.

The temperature verifications of LARM2, as in other cases, were quite successful. A comparison of observed and predicted temperatures for the Center Hill Lake simulations are shown in Tables 2.1 to 2.4. Some sensitivity was shown to input data anomalies, as would be expected. There were no measurements of velocity profiles in the reservoir, and it can only be assumed that overall circulation features were correct since the heat budget was maintained.

Center Hill Lake has a low-level outlet about 30 m below the water surface that normally withdraws hypolimnetic water. Simulations were made with an outlet at 10 m below the water surface to withdraw metalimnetic water, and for a hypothetical submerged weir upstream of the dam.

For the case of the high-level outlet Gordon (1979) concludes from LARM2 output:

(1) The hypolimnion stays much cooler throughout the simulation period, as overlying water is discharged. (Both normal and raised-outlet simulations were started with identical stratification conditions.)

(2) Discharge temperatures are considerably warmer with raised outlet.

(3) Inflow patterns continued to be the same as for the low-level outlet, with surface flows in the spring and shallow interflows during the summer.

Although certain of these conclusions might have been inferred without LARM, their demonstration is quite striking.

The submerged weir simulation was made by "zeroing out" horizontal velocities and dispersion terms along the interface between cells extending from the bottom to within 10 m of the surface. The algorithm for this change was quite straightforward and minimal. The longitudinal-vertical vector plots indicated velocities that looked like flows over a submerged weir.

Gordon (1979) expected to find temperature discontinuities on either side of the weir as the downstream volume filled with surface water over the weir. It was found, however, that since inflows were either at the surface or shallow underflows, the submerged weir had little effect on downstream temperatures.

Potomac Estuary Studies

The LARM2 hydrodynamic boundary conditions were modified to compute as an inflow, downestuary head problem with the downestuary head being a specified tide. At the tidal boundary, the vertical profile of velocity is computed using specified water surface elevations and a specified salinity profile. Salinity transport was computed in place of heat transport. The

estuarine version of LARM2 is called LAEM (Laterally Averaged Estuary Model) and has been tested for the Potomac River estuary (Edinger and Buchak, 1980).

The estuary simulations are important because estuary velocities reach easily detectable levels (on the order of 30 cm/s), and computed velocities can be compared to measured velocities. Also, water surface elevations change rapidly with time, and significant longitudinal water surface profiles develop. Reservoirs have low velocities and water surfaces that change mostly with storage. Although LARM2 has been tested on numerous occasions against measured temperature fields in reservoirs, these simulations have not provided a rigorous test of dynamic and velocity computations. Other features of stratified estuaries, such as the distribution of vertical diffusivities at different parts of the tidal cycle are well known and can be compared to computed values.

The Potomac River estuary extends 167 km from Chesapeake Bay to Great Falls, upestuary of Washington, DC. The "ocean" relative to the estuary is Chesapeake Bay, and the estuary responds to the tide height variation and vertical salinity distribution in the bay. During September 1974, hourly velocity and salinity profiles were measured at stations that were 19 and 35 km from the estuary mouth (Stations P10 and P19, respectively). Data at these stations are used for verifying the ability of LAEM to compute velocity fields.

The LAEM simulation was structured with a Δx of 9 km and layer thicknesses of 1 m. A single-period tide of 0.2 m amplitude and salinity profile were specified at the mouth. September 1974 freshwater inflows were specified at the upestuary end.

The narrowing cross-sectional geometry of the Potomac is such that the tidal amplitude generally increases in the up-estuary direction. A rapid change in geometry about 93 km from the mouth reduces the tidal amplitude to its minimum. The geometry of the estuary also modifies the phase lag as the tidal wave progresses up the estuary.

The first two properties of the estuary compared to the hydrodynamic computations are the observed tidal range and tidal phase lag. (The observed tidal ranges presented in Figure 2.1 are the maximum values that occurred independently at each station over a number of years and are not values concurrent with the predictions.) The comparisons are shown in Figures 2.1 and 2.2. The computations are presented for different values of the bottom friction Chezy coefficient. The latter is taken as a constant over the length of the estuary, although the LARM code does provide for spatially varying friction coefficients. It is found that a relatively high Chezy coefficent is generally required to reproduce the observed longitudinal variation in tidal range.

The observed and computed phase lags are compared in Figure 2.2. The phase lag is less sensitive to friction than is

tidal amplitude because phase lag is mostly a function of tidal wave speed and hence depth. The comparison of observed and computed values is an indication of how well the LAEM geometry schematization represents the real waterbody dynamically.

Comparisons of observed (+) and computed velocities at four depths for the station 35 km from the mouth are given in Figure 2.3 for two tidal cycles. The simulations were initialized over a period of ten tidal cycles. The simulations reproduce the velocity amplitudes and their decrease with depth. There are some phase shifts between observed and computed velocities due to short term wind effects not included in the model tide representation at the mouth of the estuary. The results show that the LAEM dynamics adequately reproduce rapidly varying velocity conditions.

A more stringent test for a tidal estuary is reproduction of the tidally averaged velocity. The tidally averaged velocity is often an order of magnitude smaller than the velocity amplitude and approaches velocities typically found in reservoirs. The tidally averaged velocity comparisons are shown in Figure 2.4 and show faithful reproduction. The surface reversal of observed velocities is due to wind effects not included in the simulations. An important feature of the velocity profile is the zero velocity crossing point. It is reproduced by the model.

The vertical distribution of the eddy viscosity and dispersion coefficient varies throughout a tidal cycle due to varying velocity shear relative to stationary salinity gradient. The computed dispersion coefficient profiles are shown for each tidal hour in Figure 2.5. The coefficient profiles computed by LAEM vary throughout the cycle as expected from other estuary studies. Other methods of formulation are considered in Chapter 4.

Sensitivity Tests with WES GRH Flume

LARM2 was applied to the WES Generalized Reservoir Hydrodynamics (GRH) flume in order to compare computed velocity and temperature fields with those observed during several experiments conducted in 1979. The well-controlled conditions at this facility and the ability to obtain directly measured velocity profiles made this a unique application. These comparisons resulted in sensitivity tests for scaling of dispersion parameters, the introduction of the Richardson number formulation for vertical dispersion coefficients, and the use of upstream differencing for the advection of momentum term in the longitudinal momentum balance.

The GRH flume and experiment are described in Johnson (1981). Basically, the experiment consisted of an upstream release of 16.15 °C water into the flume which was filled with 21.4 °C water. The flume was initially at rest, and flow was initiated by setting an inflow rate of 0.00063 m /s. The outflow was taken from near the bottom at the same rate as the inflow.

The LARM2 computational grid chosen by WES for simulation of the experiments was Δx^*=1.524 m and h=0.0762 m. A characteristic velocity for the flume is the outlet velocity of 0.0165 m/s. Based on a molecular kinematic viscosity of water of 1.5×10^{-6} m^2/s, the Reynolds number for a computational cell is 840, which is well within the laminar flow range. The LARM2 simulations were, therefore, based on setting the longitudinal dispersion coefficients of momentum and heat to their molecular diffusion values of $A_x = 1.5\times10^{-6}$ m^2/s and $D_x = 1.4\times10^{-5}$ m^2/s.

The numerical stability limits for the LARM2 implicit scheme based on the above dimensions are:

(1) $\Delta t < \Delta x/U = 92$ s

(2) $\Delta t < \Delta x/(2A_x) = 7.7\times10^5$ s

(3) $\Delta t < \Delta x/(2D_x) = 8.3\times10^4$ s

(4) $\Delta t < h^2/(2D_z) = 207$ s for D_z at its molecular value

Clearly, the Torrence condition given in (1) dominates the choice of time step. Note that the Courant or gravity wave speed criterion limits an explicit computational scheme to $\Delta t < 0.51$ s.

The first simulation was for A_x and D_x at their molecular values, with D_z determined from a Richardson number criterion in regions of unstable vertical density gradients. The Δt was initially taken as 60 s. In the initial time steps, the simulation immediately produced a characteristic density underflow at the head of the channel showing a velocity and temperature front moving along the bottom. As the density front velocity

* For convenience, symbols and unusual abbreviations are listed and defined in the Notation, Appendix A.

increased, however, the Torrence condition was exceeded locally and computations at a Δt=60 s were terminated. The Δt was successively lowered until the maximum computed velocity satisfied the Torrence condition. This was at a Δt=15 s, with a maximum local velocity in the wedge of 0.06 m/s.

The simulations at Δt=15 s eventually produced local temperature inversions (anomalies of 0.1 to 0.3 ^{o}C). It was obvious that the Δt was too large for local convective mixing to be completed relative to advection. The theoretical basis for this effect is found by combining relations (1) and (4) above. These anomalies were eliminated when Δt was reduced to 5 s, its final value.

The second simulation set was based on evaluating the shear stress terms from the velocity gradient and evaluating the vertical eddy viscosity from a Richardson number (Ri) criterion. For high positive values of the Ri, the lower limit to A_z was taken as the molecular value. For high negative values, the upper limit was taken as $A_z < h^2/2\Delta t$ to be compatible with condition (4) above and as used for the Richardson criterion on vertical mixing in the heat balance. These simulations showed substantially the same results as the first.

An examination of the magnitude of the individual terms in the x-direction momentum equation showed that the advection of velocity terms ($\frac{\partial uu}{\partial x}$ and $\frac{\partial uw}{\partial z}$) in the previous simulations of the flume were of the same order of magnitude as the main driving

term, the horizontal pressure gradient ($\frac{\partial \rho}{\partial x}$). These simulations were the first in which the advection terms were of such importance. The velocity fields computed in the first two simulation sets also showed the formation of prominent eddies, which were not apparent in the flume test. For these two reasons, it was decided to apply upstream differencing throughout the grid for both the $\frac{\partial uu}{\partial x}$ and $\frac{\partial uw}{\partial z}$ terms instead of only for the $\frac{\partial uu}{\partial x}$ term in the vicinity of the outlet. This change resulted in an improved time-temperature curve and more rational velocity fields.

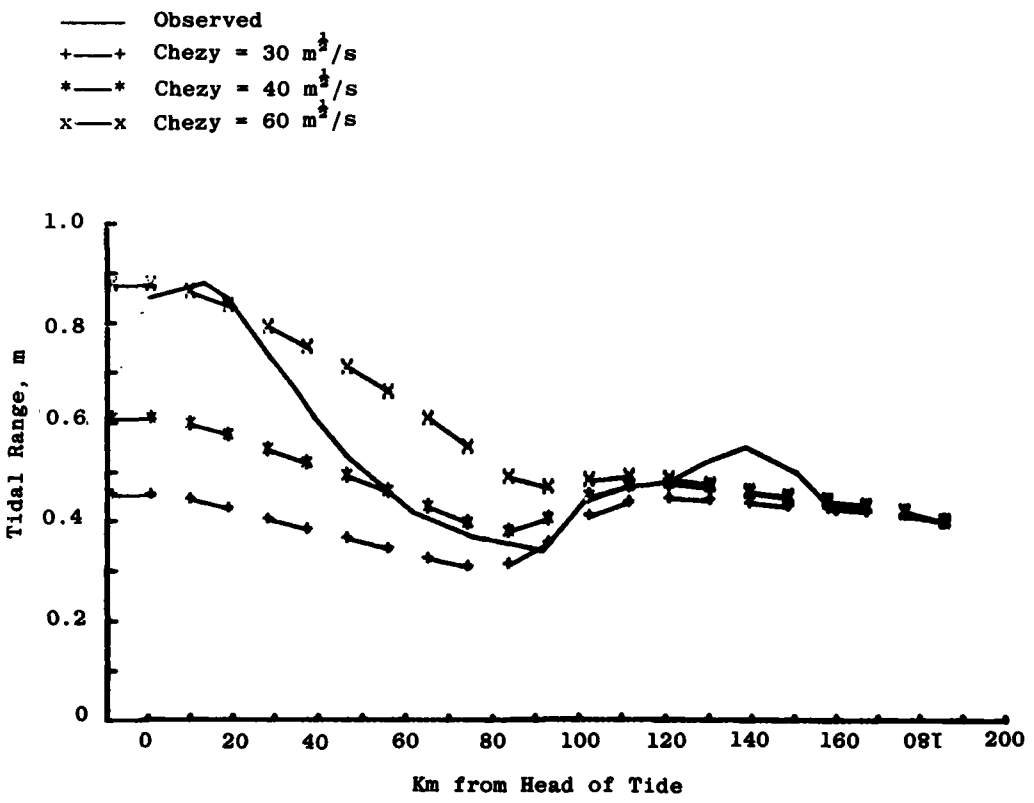

Figure 2.1

Comparison of Observed and Predicted Tidal Ranges along the Potomac Estuary

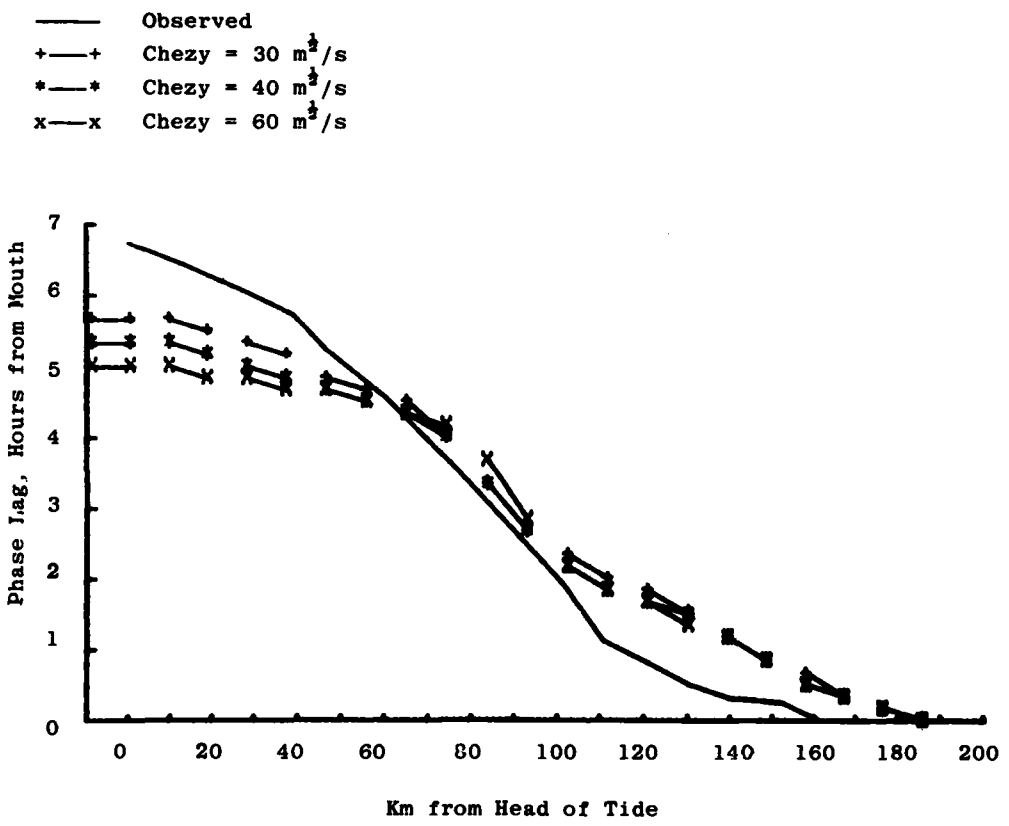

Figure 2.2

Comparison of Observed and Predicted Tidal Phase along the Potomac Estuary

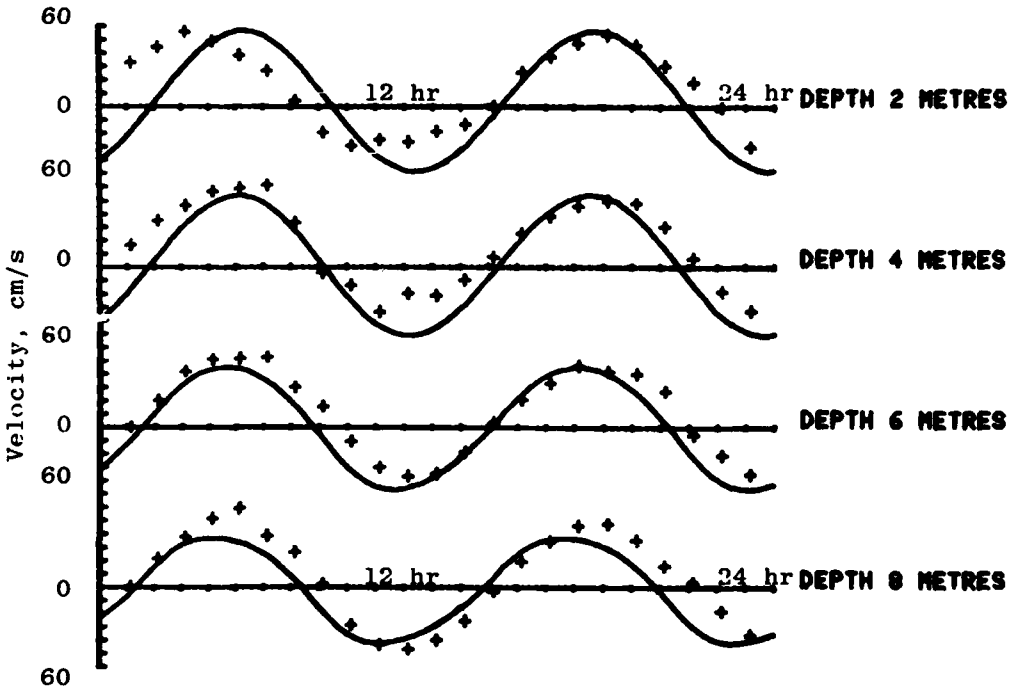

Figure 2.3

Comparison of Observed (+) and Computed Velocities 35 km from the Estuary Mouth (Station P19) for the Indicated Depths

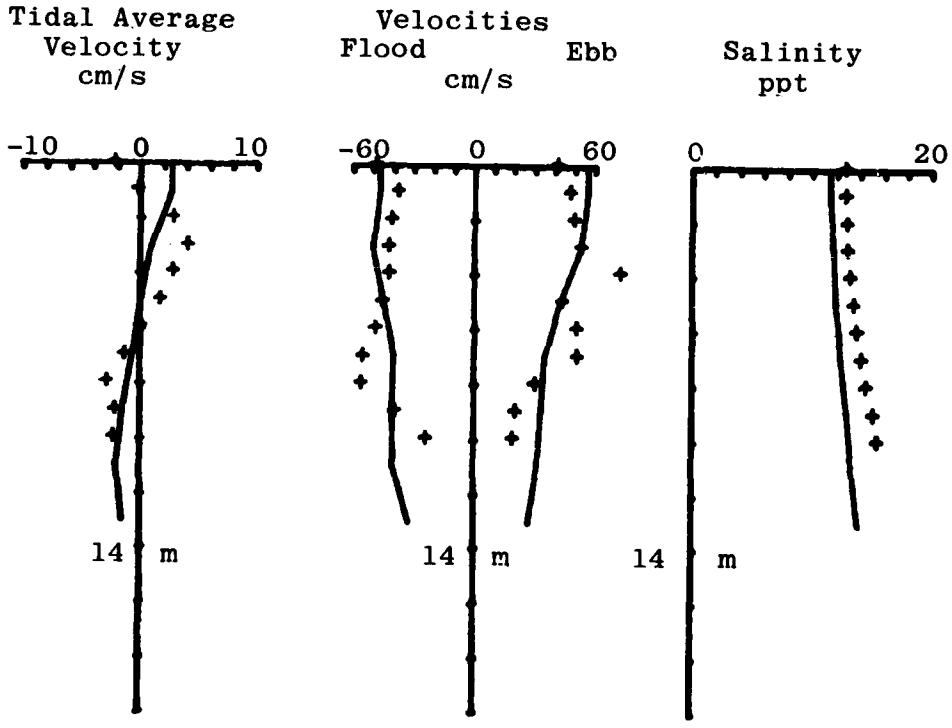

Figure 2.4

Computed and Observed (+) Tidal Averaged Velocity Profile, Maximum Ebb and Flood Velocities, and Salinity Profile at Station P19 Potomax Estuary for September 9-10, 1974

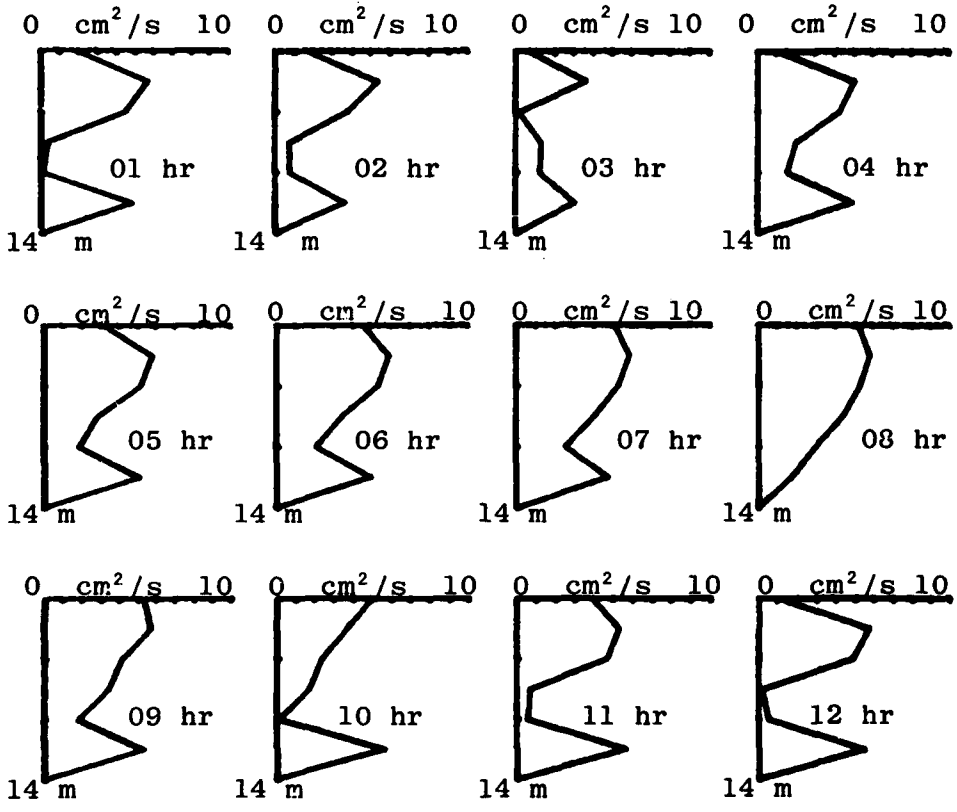

Figure 2.5

Computed Vertical Dispersion Coefficients for Station P19 Hourly through a Tide Cycle Corresponding to Velocity Profiles in Figure 2.4

TABLE 2.1 Center Hill Lake Comparison of Predicted and Observed Temperatures (°C) for April 4, 1972 (Gordon, 1979).

Depth of Sample feet	Station 2 CFRM 27.2		Station 4 CFRM 49.1		Station 5 CFRM 61.3		Station 7 CFRM 75.7	
	Predicted	Observed	Predicted	Observed	Predicted	Observed	Predicted	Observed
1.	-	10.9	-	10.9	-	11.9	-	12.5
10.	12.6	10.5	12.6	10.9	11.9	11.2	11.2	12.2
20.	10.5	10.3	10.3	10.9	10.4	11.1	10.4	11.2
30.	9.3	10.2	9.3	10.9	9.6	11.0	10.3	11.1
40.	8.7	9.8	8.7	10.8	9.0	10.9	10.3	11.1
50.	8.4	9.0	8.3	10.1	8.6	10.5	10.2	11.0
60.	8.2	8.9	8.1	9.8	8.3	10.0	10.0	10.9
70.	8.2	8.4	8.0	-	8.1	9.0	9.5	-
80.	8.1	8.0	8.0	8.3	8.0	8.3	8.9	-
90.	8.1	-	8.0	-	8.0	-	8.5	-
100.	8.0	7.9	8.0	8.1	8.0	8.0	8.3	-
110.	8.0	-	8.0	-	8.0	-	8.1	-
120.	8.0	7.9	8.0	8.0	-	-	-	-
130.	8.0	-	8.0	-	-	-	-	-
140.	8.0	7.9	8.0	8.0	-	-	-	-
150.	8.0	-	8.0	-	-	-	-	-
160.	8.0	7.9	8.0	-	-	-	-	-
170.	8.0	-	8.0	-	-	-	-	-
180.	-	-	-	-	-	-	-	-
190.	-	-	-	-	-	-	-	-
200.	-	-	-	-	-	-	-	-
Average mean error, °C	-0.07		-0.61		-0.88		-0.86	

Conditions of Prediction:

(1) Days into run sequence - 22

(2) Type of Simulation - Isothermal to spring stratification

(3) Other - Average mean error of simulation = -0.54°C

TABLE 2.2 Center Hill Lake Comparison of Predicted and Observed Temperatures (°C) for September 27, 1972 (Gordon, 1979).

Depth of Sample feet	Station 2 CFRM 27.2		Station 4 CFRM 49.1		Station 5 CFRM 61.3		Station 7 CFRM 75.7	
	Predicted	Observed	Predicted	Observed	Predicted	Observed	Predicted	Observed
1.	-	25.9	-	25.5	-	25.5	-	26.1
10.	25.5	25.9	25.5	25.6	25.5	25.5	25.3	25.9
20.	24.9	25.9	25.0	25.6	25.0	25.5	24.3	25.6
30.	22.8	25.6	22.8	24.0	22.8	24.1	22.3	23.7
40.	20.8	21.1	20.9	22.0	20.8	22.0	20.4	20.8
50.	19.4	18.8	19.4	18.5	19.4	18.9	18.9	18.0
60.	18.4	16.1	18.3	16.1	18.2	16.3	17.7	15.9
70.	17.7	14.8	17.4	15.1	17.3	15.0	16.9	14.1
80.	17.1	13.4	16.6	13.9	16.6	14.1	16.3	-
90.	15.3	12.3	15.5	12.4	15.7	13.1	15.8	-
100.	12.5	11.0	13.7	11.5	14.4	-	14.6	-
110.	11.2	10.2	11.6	-	-	-	-	-
120.	10.2	9.8	10.2	-	-	-	-	-
130.	9.6	9.4	9.5	-	-	-	-	-
140.	9.1	9.2	-	-	-	-	-	-
150.	8.8	9.1	-	-	-	-	-	-
160.	8.6	-	-	-	-	-	-	-
170.	-	-	-	-	-	-	-	-
180.	-	-	-	-	-	-	-	-
190.	-	-	-	-	-	-	-	-
200.	-	-	-	-	-	-	-	-
Average mean error, °C	+1.0		+1.6		+1.2		+0.62	

Conditions of Prediction:

(1) Days into run sequence - 134

(2) Type of Simulation - Summer stratification

(3) Other - Average mean error of simulation = +1.13°C

TABLE 2.3 Center Hill Lake Comparison of Predicted and Observed Temperatures (°C) for March 29, 1973 (Gordon, 1979).

Depth of Sample feet	Station 2 CFRM 27.2		Station 4 CFRM 49.1		Station 5 CFRM 61.3		Station 7 CFRM 75.7	
	Predicted	Observed	Predicted	Observed	Predicted	Observed	Predicted	Observed
1.	-	12.2	-	12.9	-	13.8	-	13.2
10.	12.4	12.2	12.0	12.9	11.4	12.1	11.5	12.2
20.	11.6	12.1	10.9	12.8	10.5	12.0	10.8	11.9
30.	11.1	12.0	10.4	12.8	10.1	11.8	10.6	11.8
40.	10.6	12.0	10.1	12.2	9.7	11.5	10.5	10.8
50.	10.1	11.5	9.8	12.1	9.5	11.3	10.4	10.5
60.	9.8	11.0	9.5	12.0	9.3	11.2	10.3	10.4
70.	9.6	11.0	9.1	11.5	9.1	11.0	10.0	10.2
80.	9.4	10.8	8.8	11.1	9.0	11.0	9.7	10.2
90.	9.2	-	8.4	10.6	8.9	11.0	9.2	10.2
100.	8.4	9.9	8.2	9.5	8.9	10.3	9.0	-
110.	8.2	-	8.1	8.9	8.9	-	8.8	-
120.	8.1	8.0	8.0	8.2	-	-	-	-
130.	8.0	-	8.0	8.0	-	-	-	-
140.	8.0	7.6	8.0	-	-	-	-	-
150.	8.0	-	-	-	-	-	-	-
160.	8.0	-	-	-	-	-	-	-
170.	8.0	-	-	-	-	-	-	-
180.	-	-	-	-	-	-	-	-
190.	-	-	-	-	-	-	-	-
200.	-	-	-	-	-	-	-	-
Average mean error, °C	-0.77		-1.6		-1.7		-0.56	

Conditions of Prediction:

(1) Days into run sequence - 29

(2) Type of Simulation - Isothermal to spring stratification through a large spring flood

(3) Other - Average mean error of simulation = 1.19°C

TABLE 2.4 Center Hill Lake Comparison of Predicted and Observed Temperatures (°C) for August 15, 1973 (Gordon, 1979).

Depth of Sample feet	Station 2 CFRM 27.2		Station 4 CFRM 49.1		Station 5 CFRM 61.3		Station 7 CFRM 75.7	
	Predicted	Observed	Predicted	Observed	Predicted	Observed	Predicted	Observed
1.	28.9	28.0	28.9	27.8	28.8	27.7	28.8	28.2
10.	26.6	27.9	26.6	27.6	26.6	25.8	26.4	26.2
20.	23.3	23.9	23.3	23.1	23.3	22.8	23.1	22.7
30.	21.4	21.5	21.2	22.0	21.2	21.0	20.8	21.2
40.	20.1	20.0	20.1	19.9	20.1	19.8	20.1	19.9
50.	19.3	18.0	19.4	18.9	19.5	17.9	19.8	17.8
60.	18.7	17.2	18.7	17.0	18.7	17.0	19.6	17.1
70.	18.2	16.3	18.1	16.5	18.1	16.4	18.7	16.7
80.	17.8	16.1	17.5	16.1	17.5	16.1	18.1	16.1
90.	16.7	15.9	16.7	15.8	16.7	15.9	17.4	-
100.	14.7	15.1	15.1	15.1	15.2	15.1	16.3	-
110.	13.5	13.9	13.4	13.8	-	-	-	-
120.	12.4	12.4	12.3	12.1	-	-	-	-
130.	11.7	11.4	11.7	11.5	-	-	-	-
140.	11.2	10.7	-	-	-	-	-	-
150.	10.7	10.0	-	-	-	-	-	-
160.	10.3	9.9	-	-	-	-	-	-
170.	-	-	-	-	-	-	-	-
180.	-	-	-	-	-	-	-	-
190.	-	-	-	-	-	-	-	-
200.	-	-	-	-	-	-	-	-
Average mean error, °C	0.52		0.47		0.99		1.2	

Conditions of Prediction:

(1) Days into run sequence - 51

(2) Type of Simulation - Summer stratification

(3) Other - Average mean error of simulation = +0.73°C

3. THE WATER QUALITY TRANSPORT MODULE AND CONSTITUENT SOURCE-SINK ROUTINES

The original version of LARM2 contained heat as the only constituent transported because of the dependence of the dynamics on density. Heat was transported with the laterally averaged advective-dispersive relationship in which attenuated short-wave solar radiation and surface heat exchange were included as source-sink terms. The transport relationship was solved implicitly layer by layer using the computationally efficient Thomas algorithm.

Use of LARM2 for the study of the transport of an additional constituent, residual chlorine, (Edinger and Buchak, 1978), was achieved by using the advective-dispersive transport relationship with residual chlorine source and sink terms. The computations were performed by replicating the advective and dispersive terms of the heat transport relations and writing the appropriate sources and sinks. The LARM2 simulations thus solved the transport equations twice on each time step: once for heat, and a second time for residual chlorine. Adding a complete set of transport computations for the second constituent almost doubled the computational time of a LARM2 simulation.

Studies of the LARM2 code showed that about 30% of the simulation time was devoted to the transport relationships, and most of this time was utilized in evaluating the tridiagonal transport coefficients. The computations could be made more efficient for

additional water quality constituents if the transport coefficients could be evaluated only once per iteration and used repeatedly for additional constituents.

One method studied to generalize the transport equations for additional constituents was to write them in matrix form and invert the matrix at each time step. The inverse matrix then multiplies the constituent source-sink terms to give constituent concentrations. The matrix inversion process took almost ten times the computational time for tridiagonal evaluation of the transport equation and required storage that increased as the square of the number of active cells. Standard matrix inversion algorithms also did not retain significant accuracy to maintain proper heat and mass balances.

The second and adopted method was, simply, to evaluate the tridiagonal coefficients for all lines of the reservoir grid and retain them for the successive constituent computations. This method of computation could easily be generalized to a water quality transport module (WQTM) that carries out the transport computations for each water quality constituent after evaluation of sources and sinks.

Formalization of WQTM

A formal statement of the WQTM can be derived from the laterally averaged, vertically integrated advective-dispersive transport relationship for any constituent, C, regardless of its

sources or sinks. The formalization shows that the transport coefficients need be evaluated only once, and only the source-sink terms need be evaluated for each constituent.

The laterally averaged, vertically integrated constituent transport relationship is

$$\frac{\partial}{\partial t}(BhC) + \frac{\partial}{\partial x}(UBhC) + (w_b bC)_{k+\frac{1}{2}} - (w_b bC)_{k-\frac{1}{2}}$$

$$- \frac{\partial}{\partial x}\left(D_x \frac{BhC}{\partial x}\right) - \left(D_z \frac{\partial BC}{\partial z}\right)_{k+\frac{1}{2}} + \left(D_z \frac{\partial BC}{\partial z}\right)_{k-\frac{1}{2}} = \frac{H_n\, Bh}{V} \qquad (3.1)$$

where

- b laterally averaged lake width at top or bottom of cell face (m)
- B laterally averaged lake width integrated over h (m)
- C laterally averaged constituent concentration integrated over h (mg ℓ^{-1})
- D_x x-direction temperature and constituent dispersion coefficient (m^2/s)
- D_z z-direction temperature and constituent dispersion coefficient (m^2/s)
- h horizontal layer thickness (m)
- H_n source strength (mg$\cdot\ell^{-1}\cdot$ m$^3\cdot$ s^{-1})
- k integer layer number, positive downward
- t time (s)
- U x-direction, laterally averaged velocity integrated over h (m/s)
- V cell volume ($B\cdot h\cdot\Delta x$) (m^3).
- w_b z-direction, laterally averaged velocity (m/s) (W in FORTRAN code)
- x and z Cartesian coordinates: x is along the lake centerline at the water surface, positive to the right, and z is positive downward from the x-axis (m)

In LARM2 the velocities, U and W, and dispersion coefficients, D_x and D_z, are evaluated from the hydrodynamic equations using Richardson number relationships and are available for evaluating the constituent balances. Each constituent being evaluated has a balance given by Equation 3.1, and each balance must be evaluated separately. Reactions and interactions between constituents are included in the source-sink term, H_n, which is evaluated separately from the transport equations.

For laterally averaged vertically integrated transport where the horizontal grid length is much greater than the vertical grid length, the constituent transport relationships can be evaluated layer by layer along the x-axis in an implicit finite difference formulation on an i,k grid with i horizontal and k vertical. The upwind differencing scheme used in the heat balance computation to maintain exact conservation without averaging concentrations is also applied to the constituent balance.

The implicit tridiagonal form of the transport equation is maintained by taking the longitudinal transport terms forward in time and lagging the vertical transport terms. The relationship could be expanded to an alternating-direction-implicit scheme (ADI) by evaluating the left-hand side for the x-direction terms over half a time step and then evaluating the vertical terms on the left-hand side for the second half a time step. The ADI is unnecessary in LARM2 because of the much greater size of Δx compared to h, and it is incompatible since D_z is known only at a

lagged time step and must be evaluated with the proper gradient, $\partial C/\partial z$, at that time step. A third reason for lagging the vertical transport terms is that D_z may be different from one constituent to the next, and it is easily evaluated as part of the right-hand side of the finite difference form of Equation 3.1.

The spatially implicit transport relationship can be expressed in tridiagonal form as:

$$a_i C'_{i-1,k} + v_i C'_{i,k} + c_i C'_{i+1,k} = d_i \tag{3.2}$$

for each k layer where:

$$a_i = -\frac{1}{\Delta x} A_{i-1,k}\left[(US_{i-1,k})\ U_{i-1,k} + D_{x_{i-1,k}}/\Delta x\right] \tag{3.3}$$

$$v_i = \frac{1}{\Delta t}(Bh)_{i,k} + \frac{1}{\Delta x} A_{i,k}\left[(US_{i,k})\ U_{i,k} + D_{x_{i,k}}/\Delta x\right] + \frac{1}{\Delta x} A_{i-1,k}\left[(US_{i-1,k}-1)\ U_{i-1,k} + D_{x_{i-1,k}}/\Delta x\right] \tag{3.4}$$

$$c_i = \frac{1}{\Delta x} A_{i,k}\left[(1-US_{i,k})\ U_{i,k} - D_{x_{i,k}}/\Delta x\right] \tag{3.5}$$

$$d_i = C_{i,k}(Bh)_{i,k}/\Delta t - W_{i,k}\, b_{i,k}\, C_{i,k} + W_{i,k-1}\, b_{i,k-1}\, C_{i,k-1} + D_{z_{i,k}}\, b_{i,k}\,(C_{i,k+1} - C_{i,k})/h - D_{z_{i,k-1}}\, b_{i,k-1}\,(C_{i,k} - C_{i,k-1})/h + H_n/\Delta x \tag{3.6}$$

where

$A_{i,k}$ = right cell face area = $\left[(Bh)_{i+1,k} + (Bh)_{i,k}\right]/2$

$b_{i,k} = (B_{i,k+1} + B_{i,k})/2$

$US_{i,k}$ = indicator of flow direction for upstream differencing

= 1 if $U_{i,k} > 0$, otherwise $US_{i,k} = 0$

$US_{i-1,k}$ = 1 if $U_{i-1,k} > 0$, otherwise $US_{i-1,k} = 0$

Equation 3.2 shows that each layer on the LARM2 grid has a set of four tridiagonal coefficients, a, v, c, and d, on each time step. Furthermore, three of these, a, v, and c, depend only on the velocities, geometry, and dispersion coefficients and are invariant in a time step from constituent to constituent. The transport coefficients, a, v, and c, need be evaluated only once per time step, saved, and used for all other water quality constituents. In LARM2, the transport coefficient arrays, a, v, and c, are evaluated where they are used first in the heat balance and then retained for use with the remaining water quality constituents.

The tridiagonal coefficient d is dependent on the particular constituent being evaluated. It includes the storage term or old concentrations. Secondly, it includes the two vertical transport terms, advection and mixing, which are lagged in time. Lastly, it includes the source-sink term, H_n, which must be evaluated for each constituent reaction and interaction. It is convenient to design WQTM to evaluate the d coefficient terms for each constituent over each time step and to call the tridiagonal solver (subroutine TRIDAG) for that constituent.

The FORTRAN coding of the WQTM algorithm is shown in Table 3.1. Constituent concentrations at the new time step for constituent JC are computed on each pass through the algorithm (DO loop 1820). The algorithm begins with the evaluation of the source-sink term, H_n, which is followed by the retrieving of the a, v, and c vectors from their storage arrays and the assembling of the d vector from its components, including H_n, and finally the use of the tridiagonal solution algorithm. The steps following the evaluation of H_n are performed for each layer in the grid from top to bottom. Note that the top layer d computation uses a separate set of vertical velocities that are computed from the change in mass storage in the top layer, rather than from the continuity expression around each cell in the next lower layer which is the case for the every other layer. This procedure is used to maintain perfect constituent balances and is taken from the heat balance computation.

The evaluation of H_n begins with the initialization of the H_n array, since one array is used for all constituents and the heat balance. Secondly, H_n is augmented by the reaction-interaction rates for the current constituent in terms of every other constituent and all other internal sources and sinks (decay, settling, etc.). Finally, external sources and sinks (inflows and withdrawals) are considered.

Constituent Internal Sources and Sinks

The internal sources and sinks evaluation in WQTM includes source-sink and reaction terms for each biochemical water quality

parameter being evaluated. Each constituent has reaction rates, settling velocities, etc., and interactions with other constituents that are evaluated in WQTM.

The evaluation of H_n in WQTM is based on the fact that the transport coefficients are independent of concentration (after evaluation for density-dependent terms) and that almost every constituent reaction can be written in the form:

$$\frac{\delta C1}{\delta t} = -K1C1+K2\frac{C1C2}{a+BC1} + \ldots \qquad (3.7)$$

where $\delta C1/\delta t$ represents all of the transport and storage terms about a point that are included in a, v, and c. The C1 and C2 are concentrations of constituents 1 and 2. The remaining terms are rate coefficients, cycle limits, and other terms representing reactions and interactions.

After the constituent reaction relationships are developed by the user as above, then the reaction source-sink term becomes for C1:

```
HN(I,K) = HN(I,K) + BH2(I,K)*DLX*RR(1,2)*C2(I,K,2) + ...        (3.8)
```

where RR(1,2) is the rate at which constituent 1 is transferred to constituent 2 and C2(I,K,2) is the concentration of constituent 2 at the old time level. The H_n term needs to be evaluated within the format of the LARM2 geometry computations, and this is another function of WQTM.

The user-specified portion of WQTM requires knowing the

number of constituents being considered, the rate expressions as given in the form of Equation 3.7, and how the rate parameters are evaluated. It is the last that is written into the user-defined portion of WQTM for each constituent. The procedure for assembling the user portions of the WQTM is as follows: First write the rate expressions for the problem being considered and expressions for the controlling parameters; this can usually be done in traditional format before translating to WQTM notation. Second, complete the user-specified statements. The procedure will be demonstrated for a few examples.

Example - Sediment Transport

Consider a sediment of narrow size range whose settling rate is described by a single settling velocity, Vs. The sediment may also be scoured at the bottom at a rate proportional to the adjacent horizontal velocity.

From the surface to the bottom, the local change in concentration is

$$\frac{\delta C}{\delta t} = - Vs\ \partial C/\partial z \qquad (3.9)$$

The effect of the vertical advective velocity, W(I,K), is already accounted for in the WQTM advective transport. For bottom scour and resuspension, the shear function SF is used, and for the bottom cells:

$$\frac{\partial C}{\partial t} = SF*U(I,KB) - Vs\ \partial C/\partial z \qquad (3.10)$$

The reaction-interaction sources and sinks become for the surface layer:

```
HN(I,KT) = HN(I,KT) - BH2(I,KT)*DLX*[Vs*C2(I,KT,1)]/H2(I,KT)        (3.11)
```

for the bottom layer:

```
HN(I,KB) = HN(I,KB) + BH2(I,K)*DLX*[SF*U(I,KB)]
    - Vs*[C2(I,KB,1) - C2(I,KB-1,1)/H2(I,KB)]                      (3.12)
```

and for internal layers:

```
HN(I,K) = HN(I,K)
    - BH2(I,K)*DLX*Vs*[C2(I,K,1) - C2(I,K-1,1)]/H2(I,K)            (3.13)
```

These are inserted in the WQTM routine for this constituent. WQTM then evaluates the transport of the constituent and gives the solution vector. The sediment inflow concentrations are specified as data input for evaluation of the transport source and sink contributions in WQTM.

The sediment transport internal source-sink routine is shown for a single "sediment concentration" as an example only. With the efficient transport computations as provided in WQTM, it is more realistic to compute the transport of a number of ranges of sediment sizes, each range having its specific settling velocity and bottom scour functions, and possibly interactions between size ranges. LARM2 is sufficiently flexible to include the effects of sediment concentrations on density and, subsequently, on the velocity field.

Example - Nitrogen Cycle

The constituent internal sources and sinks can be used to set up the interacting rate expressions for any number of constituents, once those expressions are known. One of the more commonly understood multiconstituent water quality processes is the nitrogen cycle in nitrogen-limiting systems. Nitrogen limiting means that there is sufficient phosphorus available so as not to control plant growth and so as to allow all stages of the nitrogen cycle to develop over a season.

One description of a seven-stage nitrogen cycle has been developed by Najarian and Harleman (1975). The cycle is shown in Figure 3.1 and has seven compartments of nitrogen (N), including (1) ammonia; (2) nitrite; (3) nitrate; (4) phytoplankton nitrogen; (5) zooplankton nitrogen; (6) particulate organic nitrogen; and, (7) dissolved organic nitrogen. The seven rate expressions for each compartment are found from the paths in Figure 3.1. They are:

ammonia:

$$\frac{\delta N_1}{\delta t} = R_{41}N_4 + R_{51}N_5 + R_{71}N_7 - R_{12}N_1 - R_{14}\frac{N_1N_4}{K_1+N_1} \qquad (3.14)$$

nitrite:

$$\frac{\delta N_2}{\delta t} = R_{12}N_1 - R_{23}N_2 \qquad (3.15)$$

nitrate:

$$\frac{\delta N_3}{\delta t} = R_{23}N_2 - R_{34}\frac{N_3N_4}{K_3+N_3} \tag{3.16}$$

phytoplankton nitrogen:

$$\frac{\delta N_4}{\delta t} = R_{14}\frac{N_1N_4}{K_1+N_1} + R_{34}\frac{N_3N_4}{K_3+N_3} - R_{45}\frac{N_4N_5}{K_4+N_4}$$

$$- (R_{41} + R_{46} + R_{47})N_4 \tag{3.17}$$

zooplankton nitrogen:

$$\frac{\delta N_5}{\delta t} = R_{45}\frac{N_4N_5}{K_4+N_4} - (R_{56} + R_{51})N_5 \tag{3.18}$$

particulate organic nitrogen:

$$\frac{\delta N_6}{\delta t} = R_{46}N_4 + R_{56}N_5 - R_{67}N_6 \tag{3.19}$$

dissolved organic nitrogen:

$$\frac{\delta N_7}{\delta t} = R_{47}N_4 + R_{67}N_6 - R_{71}N_7 \tag{3.20}$$

The transfer rates R_{ij} are complex functions of other variables, including sunlight, biomass, temperature, and even the concentration of N_1 to N_3. The transfer rates should be evaluated in WQTM ahead of the source-sink evaluation.

The growth-limiting uptake and production rates, such as the reduction of ammonia by phytoplankton $\left(R_{14} \quad N_1N_4/(K_1 + N_1)\right)$ in Equation 3.14 and its transfer to phytoplankton nitrogen in Equation 3.17, make the source-sink terms relatively complex statements. For short computational time steps, these processes can be linearized into the rate coefficients, so that the evaluation of HN(I,K) for each constituent reduces to:

```
DO JC = 1, NC
HN(I,K) = HN(I,K) + RR(JC,M)*C2(I,K,M)*BH2(I,K)*DLX
CONTINUE
```

The overall rate coefficient RR(JC,M), multiplying constituent M to get constituent JC, is summarized in Table 3.2 for each relationship, and they are evaluated prior to HN(I,K). The seven rate expressions, Equations 3.14 to 3.20, are reduced to an easily evaluated form in WQTM in terms of twenty rate expressions.

An alternative scheme is to write out each relationship of Equations 3.14 to 3.20 in WQTM for evaluation of the source-sink terms, which leads to a more lengthy expression. Since the source-sink terms are evaluated from concentrations at the previous time step, the linearized summation is equivalent.

The nitrogen cycle can be coupled to a dissolved oxygen balance that has a sink utilization by oxidation of ammonia to nitrate, as well as production and respiration by plankton. Writing the internal source-sink routine is the same for the D.O. balance as for the nitrogen balance: (1) begin with the

basic rate expressions; (2) translate to a source-sink expression for each constituent. Inflows and outflows, as well as transport through the waterbody, are evaluated in the routine WQTM following the source-sink specifications.

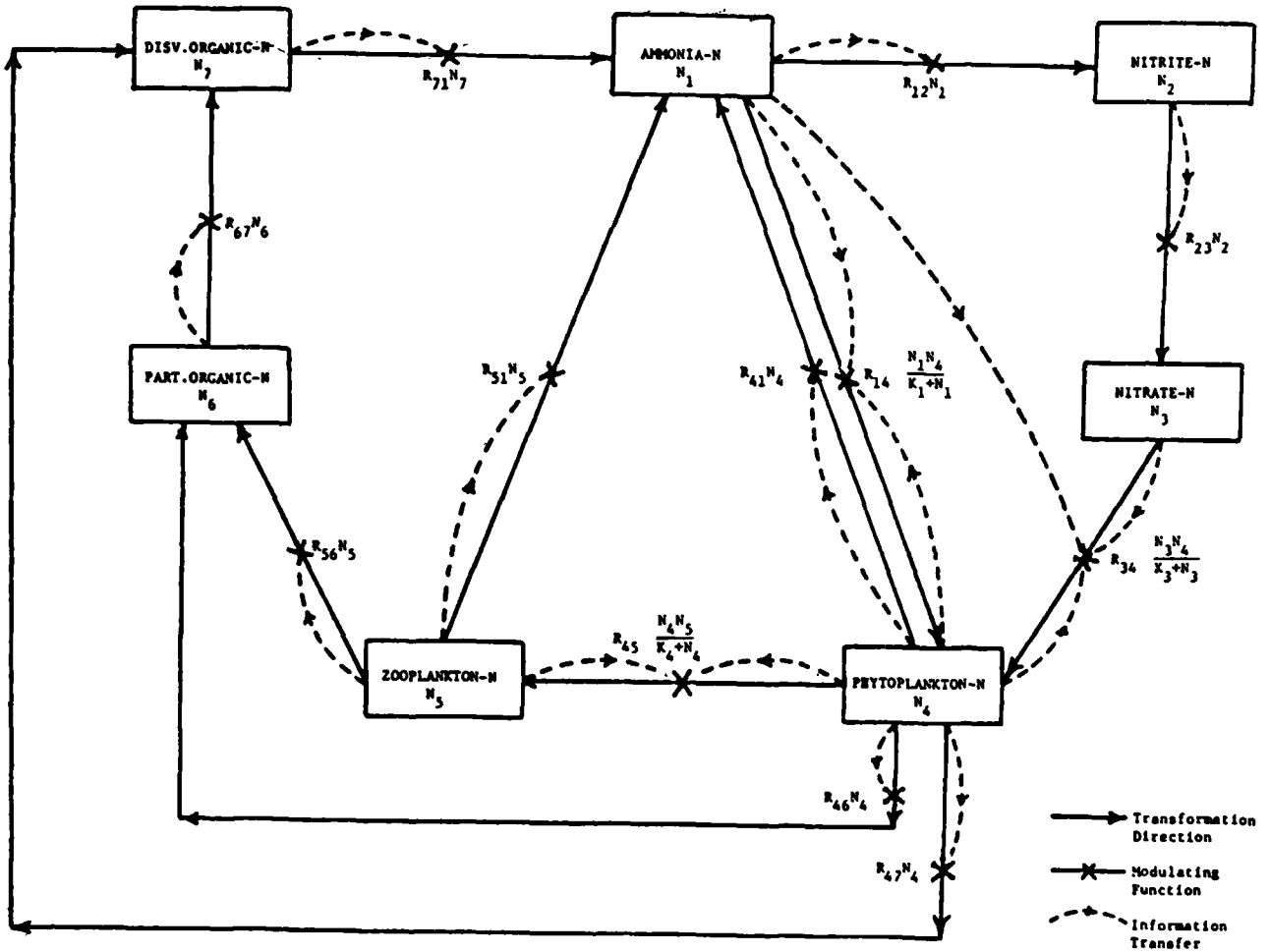

Figure 3.1

Nitrogen-Cycle Structure in Aerobic Aquatic Ecosystems (From Najarian and Harleman (1975))

TABLE 3.1 FORTRAN Coding of WQTM Algorithm in LARM2

```
C
C  COMPUTE SOURCES AND SINKS, THEN COMPUTE CONSTITUENT CONCENTRATIONS
C  FOR EACH CONSTITUENT JC
      DO 1820 JC=1,NC
C
C  INITIALIZE
        DO 1830 K=KT,KMAXM1
          DO 1830 I=IL,IMAXM1
            HN(I,K)=0.
 1830   CONTINUE
C
C  SOURCES AND SINKS DUE TO REACTIONS, MG/L M*M*M/S
        DO 1840 I=IL,IMAXM1
          KB=ISC(I)
          DO 1840 K=KT,KB
            RR(I,1)=-1.64E-7*1.09**(T2(I,K)-20.)
            DO 1840 M=1,NC
              HN(I,K)=HN(I,K)+BH2(I,K)*DLX*RR(JC,M)*C2(I,K,M)
 1840   CONTINUE
C
C  SOURCES AND SINKS DUE TO INFLOW, TRIBUTARIES, AND WITHDRAWALS
        KB=ISC(IL)
        DO 1850 K=KT,KB
          HN(IL,K)=HN(IL,K)+RLIVOL(K)*QIN*CIN(JC)
 1850   CONTINUE
        IF(NTRIB.EQ.0) GO TO 1860
        DO 1870 J=1,NTRIB
          HN(ITRIB(J),KTRIB(J))=HN(ITRIB(J),KTRIB(J))
     2    +QTRIB(J)*CTRIB(J,JC)
 1870   CONTINUE
 1860   IF(NWD.EQ.0) GO TO 1880
        DO 1890 J=1,NWD
          HN(IWD(J),KWD(J))=HN(IWD(J),KWD(J))
     2    -QWD(J)*C2(IWD(J),KWD(J),JC)
 1890   CONTINUE
```

TABLE 3.1 (continued) FORTRAN Coding of WQTM Algorithm in LARM2

```
C
C  COMPUTE CONSTITUENTS IN TOP LAYER
 1880      DO 1900 I=IL,IMAXM1
             A(I)=AS(I,KT)
             V(I)=VS(I,KT)
             C(I)=CS(I,KT)
             D(I)=C2(I,KT,JC)+BH2(I,KT)/DLT-WKY(I)*(B(I,KT+1)
       2     +B(I,KT))+(WS(I,KT)*C2(I,KT,JC)+(1.-WS(I,KT))*C2(I,KT+1,JC))
       3     /2.+DZ(I,KT)*(B(I,KT+1)
       4     +B(I,KT))*(C2(I,KT+1,JC)-C2(I,KT,JC))/(H2(I,KT)+H2(I,KT+1))
       5     +HN(I,KT)/DLX
 1900      CONTINUE
           CALL TRIDAG(IL,IMAXM1,A,V,C,D,T)
C
C  TRANSFER SOLUTION VECTOR FOR TOP LAYER TO CONSTITUENT ARRAY
           DO 1910 I=IL,IMAXM1
             C1(I,KT,JC)=T(I)
 1910      CONTINUE
C
C  COMPUTE CONSTITUENT IN REMAINING LAYERS, LAYER-BY-LAYER
           DO 1920 M=1,NLC
             IF(LC(M,1).LT.KTP1) GO TO 1920
             K=LC(M,1)
             IB=LC(M,2)
             IF(IB.LT.IL) IB=IL
             IE=LC(M,3)
             DO 1930 I=IB,IE
               A(I)=AS(I,K)
               V(I)=VS(I,K)
               C(I)=CS(I,K)
               D(I)=C2(I,K,JC)+BH2(I,K)/DLT-W(I,K)*(B(I,K+1)
       2       +B(I,K))+(WS(I,K)*C2(I,K,JC)+(1.-WS(I,K))*C2(I,K+1,JC))
       3       /2.+W(I,K-1)*(B(I,K)
       4       +B(I,K-1))+(WS(I,K-1)*C2(I,K-1,JC)+(1.-WS(I,K-1))
       5       *C2(I,K,JC))/2.+DZ(I,K)*(B(I,K+1)
       6       +B(I,K))*(C2(I,K+1,JC)-C2(I,K,JC))/(H2(I,K)+H2(I,K+1))
       7       -DZ(I,K-1)*(B(I,K)+B(I,K-1))
       8       *(C2(I,K,JC)-C2(I,K-1,JC))/(H2(I,K-1)+H2(I,K))+HN(I,K)/DLX
 1930        CONTINUE
             CALL TRIDAG(IB,IE,A,V,C,D,T)
C
C  TRANSFER SOLUTION VECTOR TO CONSTITUENT ARRAY
             DO 1940 I=IB,IE
               C1(I,K,JC)=T(I)
 1940        CONTINUE
 1920      CONTINUE
 1820    CONTINUE
```

TABLE 3.2

Summary of RR(JC,M) Coefficients for
Linear Evaluation of Nitrogen Cycle

Constituent C2(I,K,JC)

		JC→						
	Source-Sink HN(I,K)	NH_3-N N_1	NO_2-N N_2	NO_3-N N_3	Phyto-N N_4	Zoo-N N_5	PON N_6	DON N_7
	$\delta N_1/\delta t$				R_{41} -			
	NH_3-N	$-R_{12}$			$R_{14}N_1/(K_1+N_1)$	R_{51}		R_{71}
	$\delta N_2/\delta t$							
	NO_2-N	R_{12}	$-R_{23}$					
	$\delta N_3/\delta t$			$-R_{34}N_4/$				
	NO_3-N		R_{23}	(K_3+N_3)				
M ↓	$\delta N_4/\delta t$	$R_{14}N_4/$		$R_{34}N_4/$	$-(R_{41}+$	$-R_{45}N_4/$		
	Phyto-N	(K_1+N_1)		(K_3+N_3)	$R_{46}+R_{47})$	(K_4+N_4)		
	$\delta N_5/\delta t$				$R_{45}N_5/$	$-(R_{56}+$		
	Zoo-N				(K_4+N_4)	$R_{51})$		
	$\delta N_6/\delta t$							
	PON				R_{46}	R_{56}	$-R_{67}$	
	$\delta N_7/\delta t$							
	DON				R_{47}		R_{67}	$-R_{71}$

4. SPECIAL TOPICS IN LARM2 DEVELOPMENT

The examination and testing of numerous longitudinal-vertical hydrodynamics codes by Johnson (1981), including earlier versions of LARM2, have indicated a number of topics that require further consideration. These include other possible geometric configurations, refinements of the hydraulic computations, and other methods of computing turbulent mixing parameters.

The topics examined in the context of the present LARM2 development are: (1) coordinate transforms and bottom slopes; (2) variable longitudinal grids; (3) steady-state solutions; (4) channel conveyance; (5) reservoir branching; and (6) turbulence and mixing processes. The structure of the LARM2 theory, computational algorithms, coding, and development were examined to determine how the topics applied to LARM2 and how they might be accommodated.

Coordinate Transforms and Bottom Slopes

The WES GRH flume experiments with LARM2 at a very small grid size (Johnson, 1981) showed that a cold water density underflow in the sloping flume moved faster than computed by LARM2. Sensitivity analyses with LARM2 showed the computed density underflow speed to be relatively insensitive to bottom friction but highly dependent on initial inlet conditions, as are most density flow problems.

Another possible effect on the difference between the observed and computed density front speed was thought to be representation of the flume bottom slope by the step-wise vertical grid of LARM. Two methods suggested for a more explicit representation of bottom slope in longitudinal-vertical dynamics are (1) using a coordinate system transformed from the LARM2 rectangular grid, or (2) including bottom slope explicitly in the LARM2 surface wave and momentum relations rather than implicitly computing it from the grid configuration.

A transformed grid system that is approximately parallel to the bottom slope is shown in Figure 4.1. The transformed z coordinate increases with distance down the reservoir. The transformed coordinate is mapped onto the rectangular computational grid by a series of gradient relationships that would require rewriting most of the basic computations in LARM2. Mapping of waterbodies by irregular grids with transformation to a rectangular grid has been very successful in two-dimensional, vertically-mixed hydrodynamic problems. In longitudinal-vertical dynamics, it is necessary to consider the vertical variation of pressure and horizontal density gradient in the transformation. Fixed-coordinate transformations for longitudinal-vertical dynamics have not yet been tested, even for the most elementary cases.

The type of transformation shown in Figure 4.1 that would apply to longitudinal-vertical dynamics has a number of

limitations. The computations are providing extensive vertical detail at the upper end of the reservoir where it is not usually needed, and very limited vertical detail at the dam where it is usually needed. The transformed grid also provides complications in adding or subtracting grid detail as the free water surface rises and falls. In order to handle this problem, it may be necessary to use a time-varying Lagrangian grid transformation which is significantly more complex than the dynamic computations on a rectangular grid.

Bottom slope is determined in the LARM computations directly from grid geometry. Often, in fitting a given Δx-by-h grid to a waterbody, the actual bottom slope is under-or overstated at the point of the horizontal velocity computation. The manner in which bottom slope is implicitly included and how it can be explicitly stated can be shown using the primitive LARM2 relationships of horizontal momentum:

$$\frac{\partial u}{\partial t} = -\frac{1}{\rho}\frac{\partial P}{\partial x} + F \qquad (4.1)$$

where F is the sum of all other terms;
vertical momentum (hydrostatic approximation):

$$\frac{\partial P}{\partial z} = \rho g \qquad (4.2)$$

and vertical integrated continuity:

$$\frac{\partial \eta}{\partial t} + \frac{\partial}{\partial x}\int_{\eta}^{\zeta} U \, dz = 0 \qquad (4.3)$$

where η is the water surface elevation and ζ is the reservoir bottom elevation. Utilizing the vertical pressure distribution, the horizontal pressure gradient becomes:

$$-\frac{1}{\rho}\frac{\partial P}{\partial x} = g\frac{\partial \eta}{\partial x} - \frac{g}{\rho}\int_{\eta}^{z} \frac{\partial \rho}{\partial x} \, dz \qquad (4.4)$$

and is described in terms of the surface elevation as presently used in LARM2.

Direct inclusion of bottom slope in the horizontal momentum is achieved simply by writing:

$$\eta = H + \zeta \qquad (4.5)$$

where H is the total water depth. The horizontal pressure gradient becomes:

$$-\frac{1}{\rho}\frac{\partial P}{\partial x} = g\frac{\partial H}{\partial x} + g\frac{\partial \zeta}{\partial x} - \frac{g}{\rho}\int_{\eta}^{Z} \frac{\partial \rho}{\partial x} \, dz \qquad (4.6)$$

where $\partial\zeta/\partial x$ is the bottom slope. So long as $\partial\zeta/\partial x$ is determined from the grid geometry, then the horizontal pressure gradient by Equation 4.6 is identical to the LARM2 form in Equation 4.4. However, Equation 4.6 states that the bottom slope can be evaluated independently of the grid. It is then only necessary to rewrite the horizontal pressure gradient evaluation in terms of

the gradient of water column depth rather than water surface slope. The surface equation readily translates to a depth computation using $\partial\eta/\partial t = \partial H/\partial t$, and bottom slope is included as one of the forces.

Variable Longitudinal Grid

The finite difference formulations in LARM2 are presently developed for a uniform longitudinal spacing (constant Δx). Usually, in reservoir and estuary problems, the grid spacing conveniently is of the order of 1 km to 2 km. In reservoir problems such as withdrawal and pumpbacks or locations of complex tributary and geometry configurations, it is sometimes useful to have more spatial detail of the reservoir flow field and transport.

Any finite difference scheme of the momentum and transport equations can be examined for consistency by identifying the "cell" around the primary variable being computed. The momentum balance can be examined for a cell around the location of the horizontal velocity component, and the transport balance can be examined for a cell around the location of the constituent concentration. Each cell has gradient at both faces, which are the surface slope and horizontal density gradients for momentum and the advection and dispersion gradients for constituent transport.

The constituent transport relation enters the momentum balance through the horizontal density gradient. For a space-

staggered grid where constituent concentrations are computed at points between the velocities, the gradients of velocity in transport are compatible to the gradients of density in momentum when the grid spacing is uniform. The same is true for the water surface profile equation.

Unequal grid spacing requires extensive averaging of primary variables by weighting between grid points. The convenient upwind differencing on momentum and constituent advection inherently assumes a uniform grid spacing and would require a weighted form for a nonuniform grid to be compatible with continuity. It is possible to develop the finite difference forms of the relationships for an unequal grid spacing, but they must obey the same conditions of consistency, compatibility, and continuity as found for the uniform spacing.

The perceived limitations of the uniform Δx used in LARM2 can be overcome by two methods. First is to perform computations at a Δx smaller than normally used. The LARM2 computations are quite efficient in terms of computer time, yet most problems are run with 15-20 longitudinal segments and up to 25 vertical layers. The number of longitudinal segments could easily be doubled without encountering excessive computer costs.

Another method is to perform LARM2 simulations for the usual large Δx and then set up a second LARM2 simulation for a portion of the waterbody at a smaller Δx. The computed velocities, concentrations, etc., of the large-scale case become the

boundary conditions for the smaller scale case. This approach presumes there is similarity over the scales of different Δx, which there is for a uniform grid spacing.

Steady-State Solution

There are a few problems in longitudinal-vertical water-body dynamics that can be examined using steady-state solutions. Steady-state cases have steady boundary flows, steady boundary consitutent concentrations, and steady boundary exchange processes. Steady-state conditions might be specified for preliminary examination of flow fields before a complete set of time-varying boundary data is assembled. The real reservoir problem is one of time-varying unsteady inflows, outflows, and meteorological conditions.

The LARM2 computations are designed to iterate over time the sequence of the surface-wave equation, the pressure distribution, the horizontal momentum balance, internal continuity, tations can be performed for specified steady boundary conditions which are really a special case of the more general time-varying boundary conditions. For iterative solutions of the time-varying equations to steady state, the flow field establishes rather quickly, while the constituent transport takes considerably longer to establish the constituent distribution. In general, for an implicit solution, the flow field is established within two surface-wave travel times over the length of

the reservoir or estuary, while the constituent balance gets established over the residence time of the waterbody. The latter is due to the time required to build up storage of the constituent within the waterbody.

Steady-state solutions appear attractive because of the reduction in computer time. However, even if the local time change components are eliminated from the formulation of the basic equations, the solution technique must be iterative. For steady-state conditions, the LARM2 computations can be made quite efficient by eliminating the local storage term from only the constituent transport relation. It is done quite simply by eliminating the BH1(I,K)/DLT from the V(I) of the tridiagonal coefficient and T2(I,K)*BH2(I,K)/DLT term from the D(I) tridiagonal coefficient in the constituent transport equations. These changes produce the steady-state constituent balance; the computational procedures remain unchanged.

A LARM2 steady-state solution is achieved basically by computing a steady-state constituent distribution for each iteration of the flow-field dynamics. It is based on the fact that the implicitly computed flow field becomes established quite rapidly and without initialization oscillations. The computational procedure is similar to iterative solution techniques that would be required by reformulation from the steady-state form of the basic equations.

Channel Conveyance

Channel conveyance refers to the fact that a larger fraction of flow per cross-sectional area (or velocity) occurs in main channel areas than occurs in overbank areas. For LARM2 this means choosing the lateral widths to apply to the main channel area and treating the overbank areas as regions of lateral inflow and outflow. The result is generally higher velocities in the main channel area than would be obtained using widths for the whole cross section. Methods of computing the channel conveyance sections and widths are presently available in the Hydrologic Engineering Center's GEDA program, once the user has specified which channel regions are to be included in the conveyance area.

Revising LARM2 to incorporate a conveyance width and an overbank area can be performed within the existing computational structure. At each longitudinal location, an overbank planar area, AB(I,K), can be introduced which is a function of depth. Presently, a tributary inflow, QTRIB(J), is specified for each J tributary. Each J tributary has longitudinal position, ITRIB, and a vertical position, KTRIB, computed on the basis of density inflow depth. The QTRIB(J) is presently the lateral inflow to the mainstem LARM2 computations. It can be used to account for lateral inflows and outflows to and from the main flow as:

$$QTRIB(J) = QTRIB(J) - AB(I,K) \frac{\partial \eta}{\partial t} \qquad (4.7)$$

where $\partial\eta/\partial t$ is the change in water surface elevation from one time step to the next. The overbank flow computation indicated by Equation 4.7 assumes that the vertical distribution of temperature and other water quality parameters is the same in the tributary overbank area as in the mainstem area. It also assumes that the net flow into and out of the overbank area when there is no tributary inflow is due only to change in water level. The above correction allows using a more realistic conveyance width in the main LARM2 computations past mouths of tributary embayments. Larger tributary segments can be handled by branching.

Reservoir Branching

The LARM code is presently structured to compute vertical velocity and constituent profiles along a single center line, with tributary inflows and withdrawals. The case of a reservoir formed by a dam near the junction of two major tributaries has been handled successfully in LARM2 by running the model center line continuously down one arm and up the other. More dendritic reservoir geometries have a number of major branches for which it is necessary to have longitudinal and vertical resolution of the velocity and constituent fields.

The LARM2 code is presently formulated for "flow-flow" boundaries in which inflows and outflows at either end of the model are specified. The branching problem with a major branch

intersecting the mainstem reservoir is an "inflow-head" boundary problem, with inflows specified in the upper end of the branch and the water surface matched at the junction. LARM2 has been run successfully for the "inflow-head" boundary case in the estuary version, LAEM, (Edinger and Buchak, 1980). The proper form of the dynamic boundary conditions and their location in the computation are known and have been demonstrated.

Extension of LARM2 to computing dynamics in branches can be accomplished by computing on each time step the mainstem dynamics with flow-flow boundaries, then computing the flow-head dynamics for each branch using the mainstem elevation. The inflows and outflows between the tributary branch and mainstem are computed for the branch dynamic computations. These flows become tributary flows to the main branch.

The LARM computational algorithms need few changes to incorporate branching cases. The longitudinal computational limits have been generalized to a variable beginning and ending coordinate. The end coordinates can be made a function of the branch number. For a typical case the mainstem may run from I=1 to I=16, the first branch I=17 to I=28, and the second branch I=29 to I=34. This procedure allows using the present arrays of variables and computational loops. An additional coordinate is required to specify where the branches intersect the mainstem and where to apply the branch boundary head condition. The present computational structure of LARM2 is such that extension to branching problems is quite feasible.

Turbulence and Mixing Processes

The computational algorithms in LARM2 are developed to include turbulent transport dispersion coefficients and eddy viscosities as functions of time and space. The four parameters that are utilized for turbulent transport of constituent and momentum are the vertical dispersion coefficient, D_z, the vertical eddy viscosity, A_z, tne longitudinal dispersion coefficient, D_x, and the longitudinal eddy viscosity, A_x.

LARM2 utilizes the Richardson number concept to evaluate the vertical dispersion coefficient and vertical eddy viscosity as functions of buoyancy and velocity shear. It is a classical formulation disscussed in Edinger and Buchak (1980) and has the form of:

$$A_z = A_{z0} \, (1 + 10 \, Ri)^{-1/2} \tag{4.8}$$

for momentum and:

$$D_z = D_{z0} \, (1 + \frac{10}{3} \, Ri)^{-3/2} \tag{4.9}$$

for constituent transport. The Richardson number, Ri, is defined as:

$$Ri = \frac{\frac{g}{\rho} \frac{\partial \rho}{\partial z}}{(\frac{\partial U}{\partial x})^2} \tag{4.10}$$

and is the ratio of potential energy due to buoyancy to kinetic

energy being dissipated. In the classical case, A_{z_0} and D_{z_0} are taken as constants for the waterbody. The A_z and D_z vary spatially and temporally throughout the waterbody and are constrained between their molecular values (as Ri gets large) and a maximum of $h^2/\Delta t$ for the grid size scale effects. The longitudinal coefficients D_x and A_x are presently taken as constants since the solutions are insensitive to them at large scales.

The Richardson number formulation accounts for changes in turbulent dispersion and eddy viscosity under stratified conditions and is quite simple to apply. It does not, however, allow for varying A_z and D_z for unstratified conditions or for any transport of turbulent kinetic energy from one portion of the waterbody to another. Nor does it allow for similarity relations between D_x and D_z or A_x and A_z in terms of modelling scales Δx and Δz, except empirically.

Another method for relating the dispersion and viscosity parameters to the mean flow field is through the evaluation and transport of turbulent kinetic energy, K, as generated by shear and buoyancy. The turbulent kinetic energy is a scalar quantity which is transported as a constituent. For laterally averaged dynamics, the turbulent kinetic energy transport relationship is (Rodi, 1980):

$$\frac{\partial BK}{\partial t} + \frac{\partial UBK}{\partial x} + \frac{\partial WBK}{\partial z} - \frac{\partial (BA_x \partial K/\partial x)}{\partial x} - \frac{\partial (BA_z \partial K/\partial z)}{\partial z} =$$

$$BA_z(\partial U/\partial z)^2 + gB\, D_z \frac{1}{\rho}\frac{\partial \rho}{\partial z} - E \qquad (4.11)$$

where B is the lateral width. The left-hand terms are: the local change in turbulent kinetic energy, advection with the mean flow field, and turbulent transport. The right-hand side is the production of turbulent kinetic energy by mean velocity shear and by buoyancy and its dissipation, E, by viscosity.

The turbulent dispersion and eddy coefficients are related to the turbulent kinetic energy as (Rodi, 1980):

$$A_x = C_x L_x K^{1/2} \qquad (4.12)$$

$$A_z = C_z L_z K^{1/2} \qquad (4.13)$$

where C_x and C_z are constants and L_x and L_z are scale lengths related to the size of the waterbody. It is thought, (Edinger and Buchak, 1980), that L_x and L_z are related to the size of the computational grid in numerical models. A similar set of relationships holds for D_x and D_z.

Turbulent kinetic energy dissipation, E, is also related to K as:

$$E = C_E K^{3/2}/L \qquad (4.14)$$

where C_E is a constant and L is a scale length. It could also be transported similarly to K, resulting in smaller scales of dissipation.

If turbulent kinetic energy is not transported or is taken as zero, the right hand side of Equation 4.11 reduces to a Richardson number description of dissipation similar to Equation 4.8. The Richardson number formulations thus apply to steady flows with no longitudinal or vertical velocity variations. This is seldom the case in reservoir problems and never the case in tidal estuaries. The dispersion coefficient and eddy viscosity respond immediately to buoyancy and shear in the Richardson number formulation, while evaluation from turbulent kinetic energy results in time delays between the occurrence of shear and buoyancy and dispersion.

Introducing the computation of turbulent kinetic energy as generated by shear and buoyancy and dissipated by viscosity into the LARM2 code is a relatively easy task since the transport computations have been generalized in WQTM. Its use allows investigating higher-order turbulence transport relationships and examining the relationship between numerical computational grid scales and turbulent length scales.

Another value of the turbulent kinetic energy formulation is in evaluation of turbulence in surface layers due to wind shear. Use of turbulent kinetic energy transport allows wind-generated shear to be transported through the water column in a less empirical manner.

The turbulent kinetic energy transport, K, is computed on the scale of Δx, Δz, and B for a given location. Reservoir

withdrawals and pumpbacks may result in withdrawal zones or jets which are at a smaller scale and are producing or dissipating turbulent kinetic energy. These become sources or sinks of K which are incorporated in its transport computation. The turbulent kinetic energy transport formulation allows a direct method for incorporating turbulence caused by withdrawal and pumpback directly into reservoir analyses.

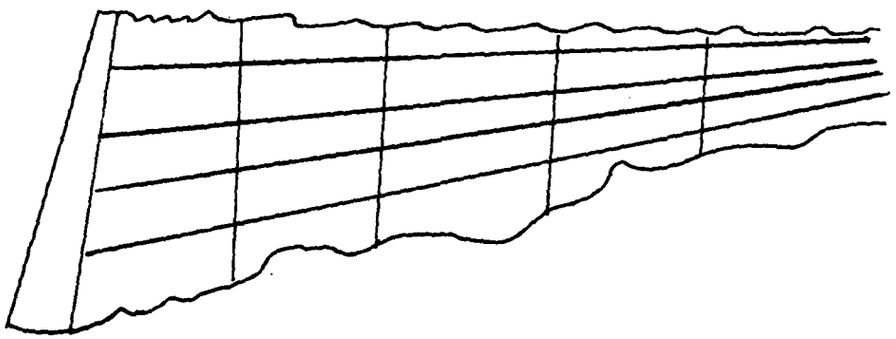

Figure 4.1

Possible Transformed Grid Representation
of Longitudinal-Vertical Reservoir Dynamics

5. RECOMMENDATIONS

Recommendations for extension of LARM2 to additional areas of study are: (1) inclusion of channel conveyance; (2) development of algorithms for reservoir branching; (3) incorporation of turbulent kinetic energy transport formulations for turbulent dispersion and eddy viscosity parameters; and (4) summarization of water quality constituent internal rate expressions into LARM2-WQTM format.

Channel Conveyance

Channel conveyance can be an important factor in reservoirs and estuaries that have extensive overbank areas and tributary embayments. Incorporation in LARM2 requires evaluation of channel conveyance widths and modification of the tributary flow routines.

Evaluation of the channel conveyance widths requires examination and possible revision of the HEC GEDA program to provide conveyance geometry and possibly to compute overbank areas as a function of elevation.

Extension of the LARM2 program requires (1) modification of the tributary inflow routines to account for changes in overbank storage and (2) modification of volume-area-elevation computations to account for overbank volumes and areas. All of these revisions can be made with the present structure of the LARM2 code.

Reservoir Branching

Reservoir Branching can be incorporated into the present LARM2 code by the addition of some computational algorithms. The head-flow type of boundary condition required for branching has been tested in the estuarine version of LARM2.

Reservoir branching will require some complex coding that will require careful testing as it is developed to assure continuity and compatibility. Also required is revision of the LARM2 print format to show longitudinal-vertical profiles in each arm.

Branching will extend the capability to map the geometry of reservoirs onto the LARM2 computations as well as give detailed velocity and constituent profiles in long tributaries.

Turbulent Kinetic Energy Transport and Mixing

The vertical and longitudinal dispersion and eddy viscocity coefficients can be evaluated in any number of ways. The present formulations in LARM2 are basically steady-state Richardson number formulations. The generalized transport code in LARM2 allows using the transport of turbulent kinetic energy from velocity shear and buoyancy as a basis for evaluating the transport processes.

Turbulent kinetic energy transport is being used for evaluation of dispersion and eddy viscosity coefficients in longitudinal-vertical estuarine dynamics. It plays the important role of transporting shear-generated turbulence away from points of generation where artifically high eddy viscocities

might be computed and inducing time lags in the velocity field. Although velocities are much lower in reservoirs than in estuaries, the vertical velocity shear can be large, particularly below the wind-driven layers.

The LARM2 code is at a level of development at which turbulent kinetic energy transport evaluation of dispersion and eddy viscosity can be introduced and tested without uncertainity of the capacility of the code to handle it. Its further development will require the design of test simulations to determine the effects of including turbulent kinetic energy transport.

Water Quality Consituent Formulations

The WQTM in LARM2 has been structured to receive the internal source/sink rate expressions for any number of interacting water quailty constituents. The latter have been illustrated for sediment transport with settling and bottom scour and for a seven-constituent nitrogen cycle. The internal source/sink computations of the WQTM are general and can be written for any set of constituent cycles and interactions for which the rate expressions are known.

The LARM2 notation used in the internal source/sink routine is quite simple; and the structure of the water quality expressions in the routine may be slightly different than in other computational schemes, such as the one-dimensional reservoir of river models. It is, therefore, recommended that the water

quality and quantitative biology routines being used in other Corps programs be abstracted and summarized in LARM2/WQTM format for use in two-dimensional reservoir problems.

There are numerous water quality cycles used in estuarine analyses and in determining the fate of pollutants that are presently not among the Corps water quality analysis procedures. These should be abstracted from the literature and made available in LARM2/WQTM format.

References

Buchak, E.M. and J.E. Edinger (1982), User Guide for LARM2: A Longitudinal-Vertical, Time-Varying Hydrodynamic Reservoir Model, Instruction Report EL-82- , prepared by J. E. Edinger Associates, Inc., for U.S. Army Engineer Waterways Experiment Station, Vicksburg, Miss.

Edinger, J.E. and E.M. Buchak (1980), Estuarine Laterally Averaged Numerical Dynamics: The Development and Testing of Estuarine Boundary Conditions in the LARM Code, prepared for U.S. Army Engineer District, Savannah, Ga.

Edinger, J.E. and E.M. Buchak (1978), Hydrodynamics and Transport of Chlorine in Panther Branch Arm, Squaw Creek Reservoir for Commanche Peak S.E.S., prepared for Texas Utilities Services, Inc., Dallas, Tex.

Gordon, J.A. (1979), Temperature and Hydrodynamic Predictions for Center Hill Lake Using the LARM Two-Dimensional Computer Model, prepared for U. S. Army Engineer District, Nashville, Tenn.

Johnson, B.H. (1981), A Review of Numerical Reservoir Hydrodynamic Modeling, Technical Report E-81-2, U.S. Army Engineer Waterways Experiment Station, Vicksburg, Miss.

Najarian, T.O. and Harleman, D.R.F. (1975), A Real Time Model of Nitrogen-Cycle Dynamics in an Estuarine System, Report No. 204, prepared for Water Resources and Hydrodynamics, Massachusetts Institute of Technology, Cambridge.

Rodi, W. (1980), "Mathematical Modelling of Turbulence in Estuaries," in Lecture Notes on Coastal and Estuarine Studies, ed. by J. Sündermann and K.-P. Holz, Proceedings of an International Symposium, held at the German Hydrographic Institute, Hamburg, August 24-26, 1978, Springer-Verlag, New York.

APPENDIX A: NOTATION

a_i, v_i, c_i, d_i	Tridiagonal matrix coefficients
A	Right or left cell face area
A_x	x-direction momentum dispersion (i.e. eddy viscosity) coefficient (m^2/s)
A_z	z-direction momentum dispersion (i.e. eddy viscosity) coefficient (m^2/s)
A_{z0}	Neutral stability z-direction momentum dispersion coefficient (m^2/s)
b	Laterally averaged lake width at top or bottom of cell face (m)
B	Laterally averaged lake width integrated over h (m)
BH	B·h (m^2); (BH1, new time level, BH2, old time level in FORTRAN code)
c	Chezy resistance coefficient, $m^{\frac{1}{2}}/s$
C	Laterally averaged constituent concentration integrated over h ($mg \cdot \ell^{-1}$)(C1, new time level, C2, old time level in FORTRAN code)
C'	Same as C but taken at the new time level
C*	Resistance coefficient
C_E	Constant in turbulent kinetic energy dissipation relation (Equation 4.14)
D_x	x-direction temperature and constituent dispersion coefficient (m^2/s)
D_z	z-direction temperature and constituent dispersion coefficient (m^2/s)
D_{z0}	Neutral stability z-direction temperature and constituent dispersion coefficient
E	Turbulent kinetic energy dissipation

F	Sum of other terms in horizontal momentum equation (Equation 4.1)
g	Acceleration due to gravity (m/s^2)
h	Horizontal layer thickness (m)(H1, new time level, H2, old time level in FORTRAN code)
H	Total depth (m)
H_n	Source strength for heat balance ($C \cdot m^3 \cdot s^{-1}$) or constituent balance ($mg \cdot \ell^{-1} \cdot m^3 s^{-1}$)(HN in FORTRAN code)
i	Integer segment number, positive to the right (I in FORTRAN code)
j,JC,M	Index to denote particular water quality constituent
J	Index to denote particular tributary
k	Integer layer number, positive downward (K in FORTRAN code)
K	Turbulent kinetic energy
K1,K2,etc.	Water quality constituent reaction rates
L	Scale lengths (related to waterbody size)
N	Nitrogen stages
P	Pressure ($Pa = N/m^2$)
R	Rate of constituent transfer, s^{-1} (RR in FORTRAN code)
Ri	Richardson number
SF	Shear function ($mg \cdot \ell^{-1} \cdot m^{-1}$)
t	Time (s)
T	Laterally averaged temperature integrated over h (^oC)
u	x-direction velocity (m/s)
U	x-direction, laterally averaged velocity integrated over h (m/s)

US	Indicator of flow direction for upstream differencing
V	Cell volume ($B \cdot h \cdot \Delta x$)(m^3)
Vs	Settling velocity (m/s)
w	z-direction velocity (m/s)
w_b	z-direction, laterally averaged velocity (m/s) (W in FORTRAN code)
W_a	Wind speed (m/s)
x and z	Cartesian coordinates: x is along the lake center line at the water surface, positive to the right, and z is positive downward from the x-axis (m)
Δx	Horizontal spatial step (m) (DLX in FORTRAN code)
ζ	Reservoir bottom elevation (m)
η	Surface elevation (m)
ρ	Density (kg/m^3)

In accordance with letter from DAEN-RDC, DAEN-ASI dated 22 July 1977, Subject: Facsimile Catalog Cards for Laboratory Technical Publications, a facsimile catalog card in Library of Congress MARC format is reproduced below.

Edinger, John E.
Developments in LARM2 : A longitudinal-vertical, time-varying hydrodynamic reservoir model / by John E. Edinger and Edward M. Buchak (J.E. Edinger Associates, Inc.) -- Vicksburg, Miss. : U.S. Army Engineer Waterways Experiment Station ; Springfield, Va. ; available from NTIS, 1982.
66 p. in various pagings : ill. ; 27 cm. -- (Technical report ; E-83-1)
Cover title.
"January 1983."
Final report.
"Prepared for Office, Chief of Engineers, U.S. Army under Contract No. DACW-78-C-0057 (Work Unit 31593; Task IA.4)."
"Monitored by Hydraulics Laboratory, U.S. Army Engineer Waterways Experiment Station."
At head of title: Environmental & Water Quality Operational Studies."
Includes bibliography.

Edinger, John E.
Developments in LARM2 : A longitudinal-vertical : ... 1982.
(Card 2)

1. Computer programs. 2. Hydrodynamics. 3. LARM2 (Computer program). 4. Mathematical models. 5. Reservoirs. 6. Water quality. I. Buchak, Edward M. II. J.E. Edinger Associates, Inc. III. United States. Army. Corps of Engineers. Office of the Chief of Engineers. IV. Environmental & Water Quality Operational Studies. V. U.S. Army Engineer Waterways Experiment Station. Hydraulics Laboratory. VI. Title VII. Series: Technical report (U.S. Army Engineer Waterways Experiment Station) ; E-83-1.
TA7.W34 no.E-83-1

END

FILMED

3-83

DTIC